



**Fermi National Accelerator Laboratory**

**FERMILAB-Conf-95/094**

## **QCD at DØ and CDF**

Gerald C. Blazey

*Fermi National Accelerator Laboratory  
P.O. Box 500, Batavia, Illinois 60510*

May 1995

Presented at the *Les Rencontres de Physique de la Vallée D'Aoste, Results and Perspectives in Particle Physics*,  
La Thuile, Aosta Valley, March 5-11, 1995

## **Disclaimer**

*This report was prepared as an account of work sponsored by an agency of the United States Government. Neither the United States Government nor any agency thereof, nor any of their employees, makes any warranty, express or implied, or assumes any legal liability or responsibility for the accuracy, completeness, or usefulness of any information, apparatus, product, or process disclosed, or represents that its use would not infringe privately owned rights. Reference herein to any specific commercial product, process, or service by trade name, trademark, manufacturer, or otherwise, does not necessarily constitute or imply its endorsement, recommendation, or favoring by the United States Government or any agency thereof. The views and opinions of authors expressed herein do not necessarily state or reflect those of the United States Government or any agency thereof.*

# QCD at DØ and CDF

Gerald C. Blazey

*Fermi National Accelerator Laboratory, Batavia, IL*

## Abstract

Selected recent Quantum Chromodynamics (QCD) results from the DØ and CDF experiments at the Fermilab Tevatron are presented and discussed. The inclusive jet and inclusive triple differential dijet cross sections are compared to next-to-leading order QCD calculations. The sensitivity of the dijet cross section to parton distribution functions (for hadron momentum fractions  $\sim 0.01$  to  $\sim 0.4$ ) will constrain the gluon distribution of the proton. Two analyses of dijet production at large rapidity separation are presented. The first analysis tests the contributions of higher order processes to dijet production and can be considered a test of BFKL or GLAP parton evolution. The second analysis yields a strong rapidity gap signal consistent with colorless exchange between the scattered partons. The prompt photon inclusive cross section is consistent with next-to-leading order QCD only at the highest transverse momenta. The discrepancy at lower momenta may be indicative of higher order processes imparting a transverse momentum or “ $k_T$ ” to the partonic interaction. The first measurement of the strong coupling constant from the Tevatron is also presented. The coupling constant can be determined from the ratio of  $W + 1jet$  to  $W + 0jet$  cross sections and a next-to-leading order QCD calculation.

# 1 Introduction

During the 1992-1993 data run of the Fermilab Tevatron Collider the DØ [1] and CDF [2] detectors recorded 13 and 19  $pb^{-1}$  of data, respectively, at  $\sqrt{s} = 1.8$  TeV. The large total luminosities provided large samples of final state jets, photons, and  $W$  and  $Z$  bosons. Subsets of these data populate unexplored regions of phase space. In particular, the final state jets approach pseudo-rapidities ( $\eta$ ) of four and transverse energy ( $E_T$ ) between 10 and 450 GeV. These rich data sets, in concert with new and accurate next-to-leading order (NLO) calculations [3],[4],[5] and all order resummation calculations are posing new, rigorous, and interesting tests of QCD.

The inclusive jet cross section and NLO QCD calculations are in reasonable agreement over nearly all  $E_T$  and  $\eta$ . (However, intriguing discrepancies are evident at the highest momentum transfers.) Since the triple differential cross section is likewise well described by NLO QCD, information about the parton distribution functions (pdf's) can be deduced from the correlations implicit in the cross section. This direct measurement of the gluon structure function,  $G(x)$ , bears a striking complementarity to very low  $x_{Bj} \equiv x$  measurements of  $G(x)$  at HERA [6].

Higher order and non-perturbative predictions and associated measurements are providing new avenues for understanding jet production. This is clearly demonstrated by studies of jet production at large rapidity separation. The observation of rapidity gaps and the measurement of decorrelation between widely separated jets at the Tevatron, interesting studies in their own right, are proving to be very complementary to related measurements at HERA.

The last two results discussed in this paper are the inclusive photon cross section and a measurement of  $\alpha_s$  from  $W + jet$  production, both at  $\sqrt{s} = 1.8$  TeV. The photon cross section is in agreement with perturbative NLO QCD only at the highest  $E_T$ . In fact, a compilation of photon production measurements from the last decade show a systematic disagreement at the lowest  $x$  values. As suggested by the CTEQ collaboration [7] this may be indicative of higher order processes manifested as partonic " $k_T$ ". The  $\alpha_s$  measurement capitalizes on recent NLO  $W + jet$  calculations to deduce the first measurement of the strong coupling constant from the Tevatron [8].

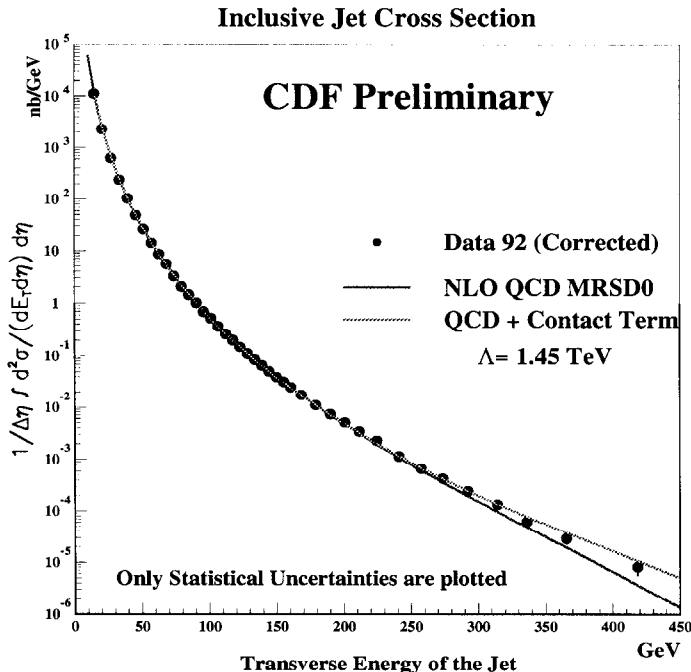


Figure 1: The central inclusive jet cross section. The solid lines are a NLO prediction without and with a contact term to model quark compositeness.

## 2 Inclusive Jet Production

At central pseudorapidities,  $|\eta| < 1$ , and over a wide range of energies,  $0.063 \text{ TeV} < \sqrt{s} < 1.8 \text{ TeV}$ , the inclusive jet cross section,  $\sigma(p\bar{p}) \rightarrow jet + X$ , is described qualitatively by leading order,  $O(\alpha_s^2)$ , QCD [9], [10], [11]. At  $\sqrt{s} = 0.63 \text{ TeV}$  and  $1.2 < |\eta| < 2.0$  the measured cross sections are in poor agreement with leading order QCD [10]. Leading order comparisons include a 30 – 50% theoretical normalization uncertainty. Recent next-to-leading order,  $O(\alpha_s^3)$ , calculations reduce the theoretical uncertainties to  $\sim 5\%$  [3], [4], [12]. The improvement can be attributed to greater stability of the calculation with respect to the renormalization scale and to improved concurrence of jet algorithms at the experimental and theoretical level [3].

Figure 1 shows the 1992-1993 central inclusive jet cross section as measured by CDF for  $0.1 < |\eta| < 0.7$  using the fixed cone jet algorithm of radius 0.7 [13]. On the logarithmic scale, next-to-leading order QCD agrees with the data (shown with statistical errors only) over nine orders of magnitude. The NLO calculation is sensitive only at the 10–20% level to the input pdf. The calculation shown in Fig. 1 incorporates the MRSD0' distribution. The percentage difference as a function of  $E_T$  between the data and theory is shown in Fig. 2. Note the excellent agreement between 10 and 200 GeV/c. Above 200 GeV/c there seems to be an excess of jet production nearly equal to the systematic error. By comparing

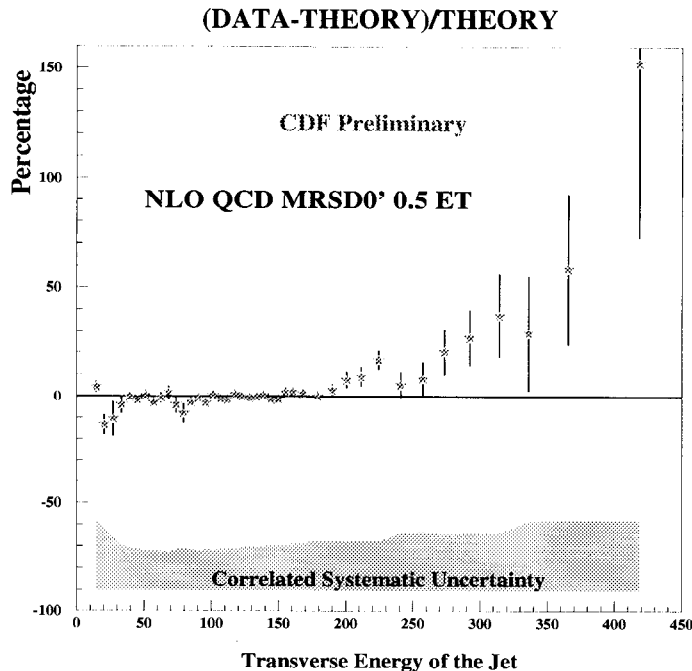


Figure 2: Difference between data and NLO QCD for the central inclusive jet cross section.

the observed production to that predicted by several quark compositeness models, CDF sets a 1.45 TeV lower limit on the quark compositeness scale. The current 1994-1995 collider run will prove interesting should the high  $E_T$  excess gain significance.

Figure 3 shows the  $D\bar{D}$  inclusive cross section for four regions of rapidity also using a 0.7 fixed cone algorithm [14]. Systematic errors are indicated by the dashed lines and the NLO calculation (using CTEQ2M) by the solid lines. As can be seen, the NLO prediction is in good agreement at all rapidities. Unfortunately, due to systematic errors, the  $D\bar{D}$  data can not yet shed light on CDF's observed excess at the highest transverse momenta. The general agreement between the data and NLO calculations over a wide range of  $E_T$  and  $\eta$  indicate that the perturbative calculations describe the partonic interactions. As shown in the next section, a more stringent NLO test is provided by the correlations between final state jets.

### 3 The Triple Differential Cross Section

In addition to testing NLO predictions, jet production at the Tevatron, dominated by gluon-gluon scattering, should provide new constraints to the gluon distribution functions. At leading order only two final state jets are produced; thus, at a *fixed* jet transverse momentum the jets have a kinematic rapidity limit simply due to energy conservation.

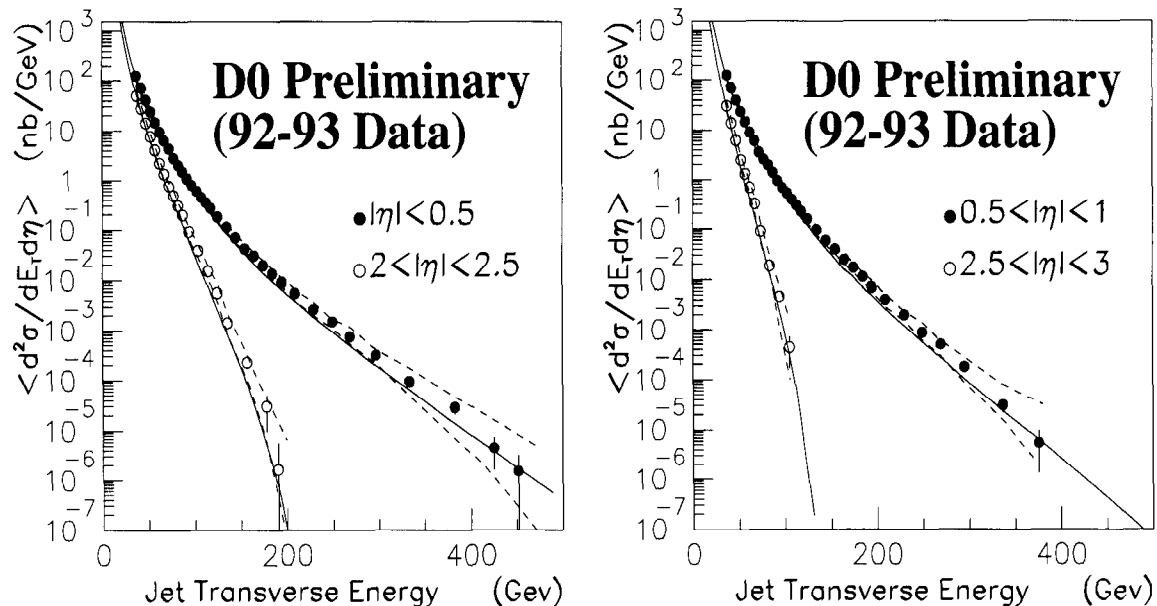


Figure 3: The inclusive jet cross section at several rapidities. The solid lines are a NLO QCD prediction and the dashed lines indicate systematic errors.

For example, at a beam energy of 900 GeV and a transverse momentum ( $p_T$ ) of 165 GeV/c the maximum possible absolute jet rapidity is slightly less than three. At NLO, this kinematic constraint is lifted. If the forward parton or jet radiates, then the second leading jet's rapidity can exceed the leading order limit. A straightforward test, then, of NLO jet calculations is to examine the rapidity correlations between the leading  $E_T$  final state jets.

If NLO theory is an adequate description of jet production, the dijet cross sections will provide information on the pdf's. This determination was first attempted at the  $Spp\bar{S}$  using the leading order (LO) single effective subprocess approximation limited to moderate values of parton  $x$  [15]. Measurement of high rapidity final state jets is necessary for reaching the very small, and the very large, values of  $x$ . At leading order, a final state with two far-forward jets can occur only if one initial parton has large  $x$  and the other small  $x$ . The resulting inequality in momentum boosts the entire event forward. Both the DØ and CDF detectors have complete calorimetric coverage up to rapidities of four [1],[2].

The triple differential cross section,  $d^3\sigma/dE_T d\eta_1 d\eta_2$ , with the leading  $E_T$  jet enumerated as jet one and the second leading jet as jet two, must be integrated over at least one variable for graphical representation. Figure 4 shows the leading jet  $E_T$  spectra with a central leading jet,  $|\eta_1| < 1.0$ . The four curves correspond to various rapidity ranges for

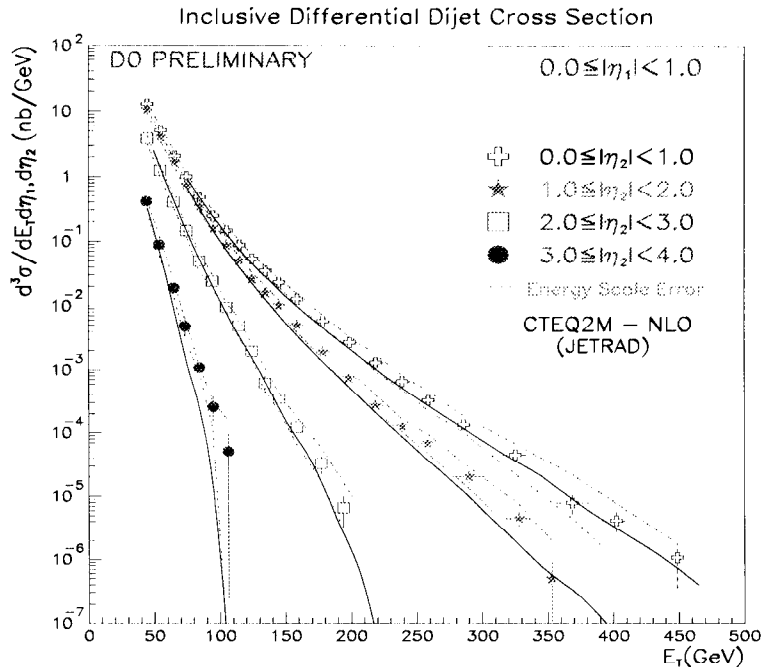


Figure 4: Leading jet  $E_T$  spectra with the leading jet central and the second leading jet at various rapidities. The dashed lines indicate the systematic errors. The solid line is a NLO prediction.

the second jet (from  $|\eta_2| < 1.0$  to  $3.0 < |\eta_2| < 4.0$ ). Within errors the  $D\bar{O}$  and CDF data are in agreement [13],[16]. As with the inclusive cross section discussed previously, the dashed lines indicate systematic errors and the solid line the NLO prediction [4]. The prediction, although generally low, agrees with the preliminary data, within errors, except at the highest rapidities where higher order corrections may become important. For reference, the LO prediction is one order of magnitude below the NLO prediction at  $E_T = 200$  GeV and  $2.0 < |\eta_2| < 3.0$  and two orders below at  $E_T = 90$  GeV and  $3.0 < |\eta_2| < 4.0$ . NLO is clearly preferred over LO.

Figure 5 shows a lego plot of the triple differential cross section with the leading jet  $E_T$  integrated over 45 to 55 GeV [16]. The cross section is given in nanobarns per GeV for the entire  $\eta_1 - \eta_2$  plane. Note the sharp fall-off at large rapidities which is due mostly to the lack of gluons at high  $x$ . Another representation of the triple differential cross section is given in Fig. 6. In addition to integration over leading jet  $E_T$  the leading jet is also held to central rapidities [16]. The figure is not quite a simple slice of the lego plot since jets with the same rapidity sign are plotted on the positive abscissa and jets with opposite rapidity sign on the negative abscissa. This plotting technique has been named the “signed distribution”. The data, indicated by the closed circles, are in excellent agreement with a NLO prediction. The dashed lines indicate the systematic errors. The

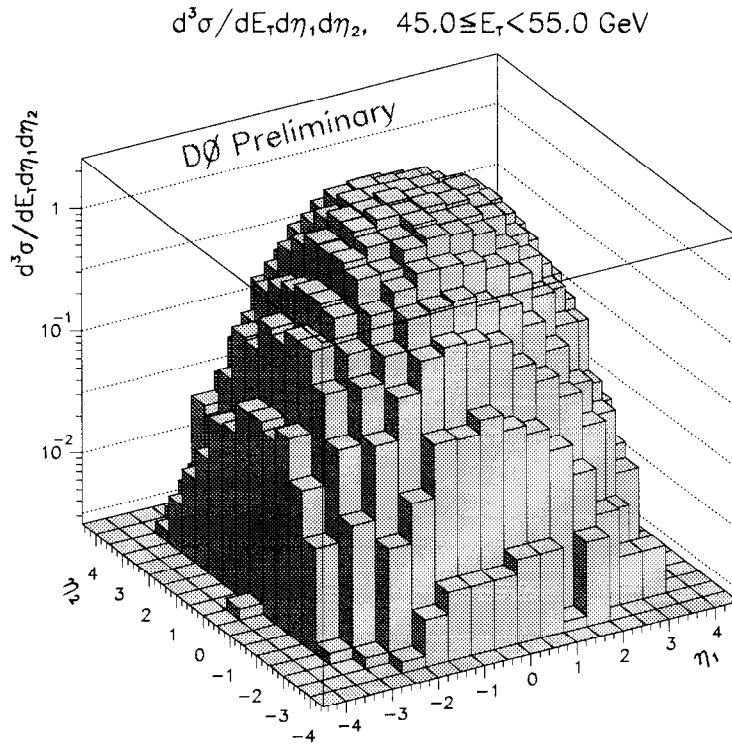


Figure 5: Lego plot of the triple differential cross section with the leading jet  $E_T$  between 45 and 55 GeV.

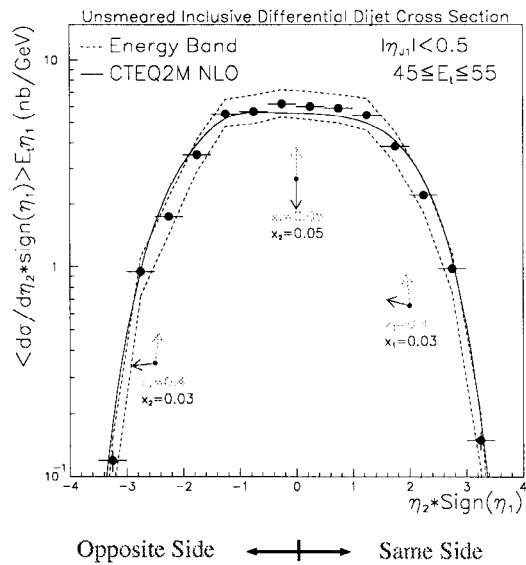


Figure 6: A “Signed Slice” of the preliminary triple differential cross section. The dashed lines represent systematic errors and the solid line a NLO prediction.

CDF collaboration has opted to investigate the triple differential cross section using yet another method based on the ratio of jets of same sign rapidity to jets of opposite sign rapidity [13]. This technique promises good sensitivity to the low  $x$  gluon content of the pdf's and is discussed later in these proceedings by David Kosower and in the references [4].

Both the inclusive and triple differential jet cross sections are fairly well described by NLO calculations. Thus, a comparison of the triple differential cross section to NLO predictions should discriminate between the various pdf's. The DØ collaboration has performed a goodness-of-fit test between the data shown in the lego plot of Fig. 5 and NLO predictions based on the CTEQ and MRS families of pdf's. The fits incorporated each bin in the  $\eta_1 - \eta_2$  plane and included systematic errors for both the data and theoretical prediction. The overall normalization was allowed to float to minimize errors due to the jet energy scale, luminosity uncertainty, and theoretical uncertainty from the choice of renormalization scale. Preliminary fit results for  $|\eta| < 2.0$  (systematic errors due to triggering and reconstruction efficiency and theoretical jet finding have yet to be incorporated) favor the CTEQ2MF and MRSD0' distributions. The greatest differences in the cross section due to pdf variations occur when at least one of the jets occupies a large rapidity region ( $|\eta| > 1.5$ ).

When compared to currently favored pdf's (CTEQ2M and MRSD-) the two best fit distributions actually require increased gluonic content for  $x < 0.3$  and decreased content for  $x > 0.3$ . Recent theoretical publications differ on this point, advocating in one instance more gluons in the general region of  $x = 0.3$  and in another instance less [4],[17]. More time and data are required to make further distinctions. The determination of the gluon structure function in the intermediate region and large  $Q^2$  is complementary to HERA measurements which are limited to very low  $x$ ,  $10^{-4}$  to  $10^{-2}$ , at low  $Q^2$  [6]. Because of the availability of NLO calculations, dijet production is once again contributing in a timely fashion to the determination of  $G(x)$ .

## 4 Jets at Large Rapidity Separation

### 4.1 Decorrelation of Jets at Large Rapidity

Dijet production at large rapidity separation offers a new test of strong interactions. Specifically, since the interjet interval may be filled with multiple gluon emission the effects of these higher order contributions on dijet correlations can be observed. Del Duca and

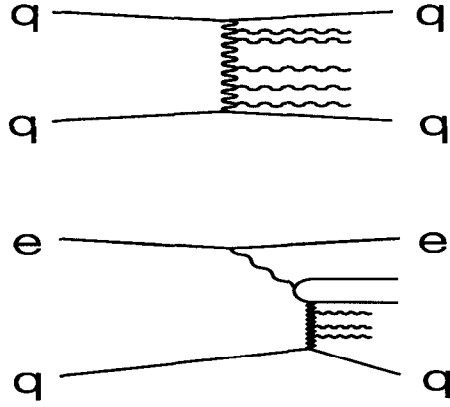


Figure 7: Diagrams illustrating high order gluon emission. The top plot represents dijet production at the Tevatron and the lower plot similar gluon emission at HERA.

Schmidt [5] and, independently, Stirling [18] have suggested that as the rapidity interval increases, logarithms involving the two energy scales describing the jet production,  $\hat{s} \gg Q^2$ , become quite large. These logarithmic terms, corresponding to gluon emission between the initial partons (top diagram Fig. 7), can be resummed using the Balitsky, Fadin, Kuraev, and Lipatov (BFKL) formalism [5],[18]. As shown in the lower diagram of Fig. 7, this exchange process is remarkably similar to electron-proton deep inelastic scattering at very low  $x$ , where the virtual photon creates a  $q\bar{q}$  pair which then exchanges a gluon with the proton. (It is interesting to note that BFKL resummation tests can be done at both HERA and the Tevatron.) Alternately, the multiple gluon emission could be modelled using angular ordering of final state radiation. Angular ordering serves to limit soft gluon radiation to regions near the initial and final state parton directions and is an approximation to the widely tested Gribov, Lipatov, Altarelli, and Parisi (GLAP) evolution. A popular implementation of angular ordering is the HERWIG fragmentation simulation [19]. The two resummations differ in the graphs or terms incorporated into the calculations.

In either case, the population of the interjet interval by multiple gluon emission should decorrelate the  $p_T$  and azimuthal angle ( $\phi$ ) of the leading two jets. At leading order there are only two final state jets which are perfectly correlated in transverse momentum and azimuthal angle. That is,  $p_{T1} = p_{T2}$  and  $|\phi_1 - \phi_2| = \pi$ . At higher orders, where the most

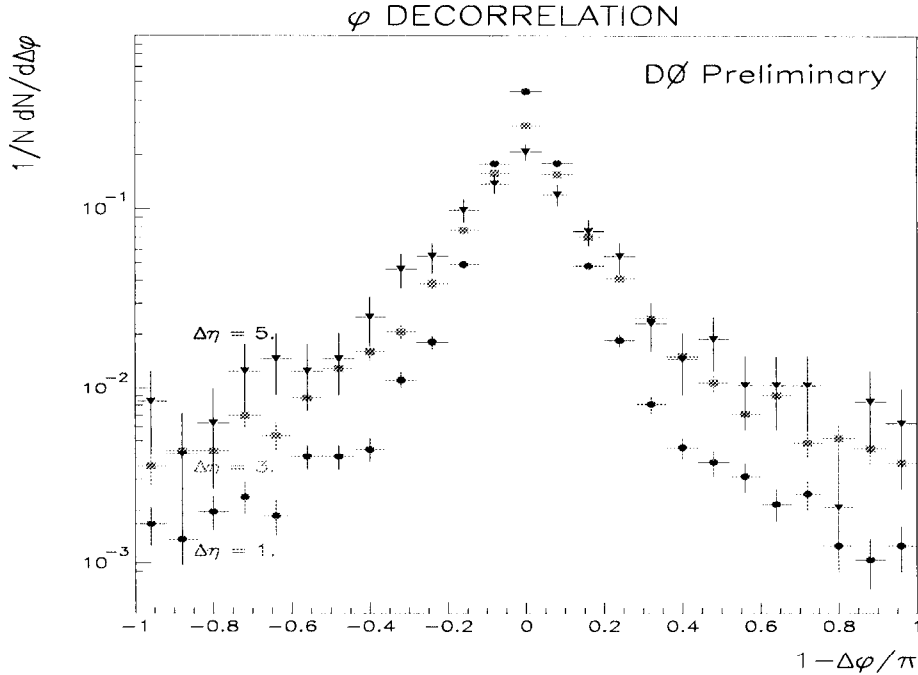


Figure 8: The correlation between leading rapidity jets. The circles are for a rapidity separation of one and the triangles for a separation of five.

forward jet is labelled jet one, and the most backward jet labelled jet two; the  $p_T$  and  $\phi$  correlations of these two jets will be weakened by additional radiation or multiple gluon emission into the interval. (Note this rapidity ordering of the jets is a departure from the traditional  $E_T$  ordering.)

The degree of decorrelation indicates the importance of the higher order processes. As mentioned earlier, at LO the correlation will be perfect, but at NLO the presence of a third parton will serve to decorrelate the leading rapidity jets, and at all orders the decorrelation will be maximal. In a similar manner, as the rapidity separation ( $\Delta\eta = \eta_1 - \eta_2$ ) increases, the decorrelation should increase since there is more phase space available for interjet gluon emission.

In Fig. 8, a preliminary result from DØ clearly shows increasing decorrelation as rapidity separation increases. The histogram plots the frequency of  $1 - \Delta\phi/\pi$  with  $\Delta\phi = |\phi_1 - \phi_2|$  for the leading rapidity jets as a function of  $\Delta\eta$ . If the two jets are perfectly correlated then every entry will be at  $1 - |\phi_1 - \phi_2|/\pi = 0$ . In contrast, if the two jets are completely decorrelated, the histogram will be populated uniformly. Note that the distribution becomes markedly less peaked as  $\Delta\eta$  increases from 1 to 5. To avoid reconstruction and trigger bias the minimum jet  $E_T$  was 20 GeV and either the forward or the backward jet minimum  $E_T$  was 50 GeV. For more details consult the references [20].

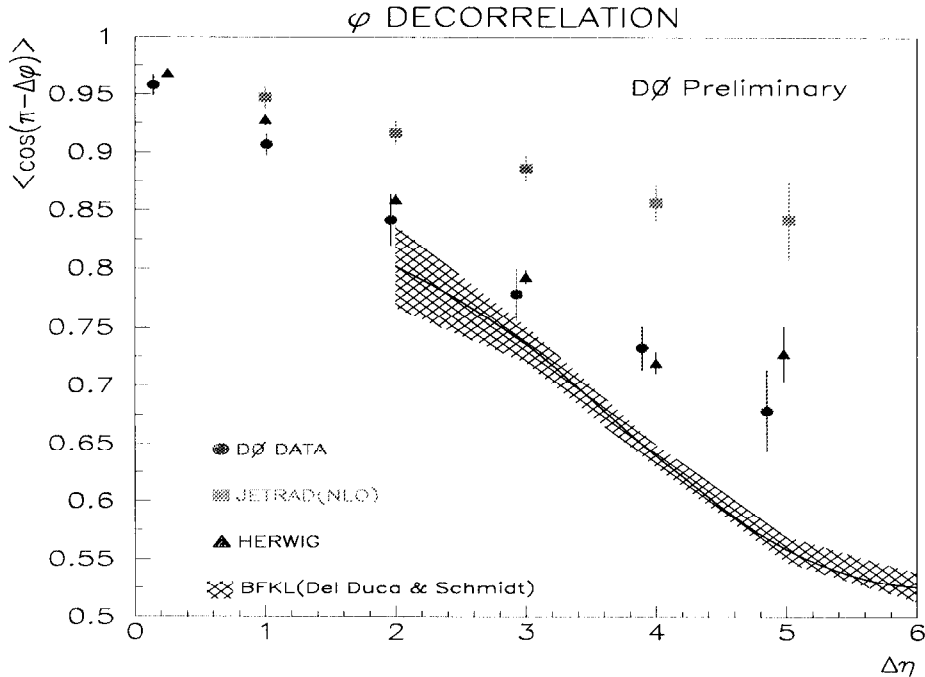


Figure 9: The decorrelation of leading rapidity jets as a function of rapidity separation. The data fall between NLO QCD and BFKL resummation calculations. HERWIG provides the best description of the data.

As shown in Fig. 9, the expectation value  $\langle \cos(\pi - \Delta\phi) \rangle$  provides a single measure of decorrelation as a function of  $\Delta\eta$ . If the jets were perfectly correlated,  $\langle \cos(\pi - \Delta\phi) \rangle$  would be unity. On the other hand, if the jets were completely uncorrelated the expectation value would be zero. Figure 9 includes three different theoretical calculations: The NLO prediction from JETRAD (which incorporates a maximum of three final state jets) shows insufficient decorrelation at all rapidities. The BFKL all orders resummation predicts too much decorrelation at all rapidities. In contrast, the HERWIG Monte-Carlo (GLAP evolution) describes the data quite well. These results are preliminary as work remains to estimate the hadronization corrections (expected to be small) between the data and theory. In any event, the decorrelation measurements are already providing information as to the dominant higher order processes in jet production.

## 4.2 Rapidity Gaps

Events with jets at large rapidity separation with no radiation between them, the so called “rapidity gaps”, signal the presence of colorless exchange between the initial partons [21]. (Contrary to the *inclusive* decorrelation measurement just discussed, a rapidity gap analysis requires a more *exclusive* final state with large rapidity separation.) In the case

of color-singlet exchange, radiation at central rapidities is suppressed; but, for color-octet gluon exchange the interjet rapidity interval is easily populated by soft radiation [22]. Colorless exchange could involve the photon, heavy vector bosons, or the Pomeron. In a QCD model the Pomeron consists of two gluons in a color-singlet state. Relative to single gluon exchange, electroweak and Pomeron exchange are suppressed by three and one orders of magnitude, respectively [23],[24].

Ordering jets by  $E_T$ , the rapidity separation of an event is given by the cone edge separation of the two leading jets,  $\Delta\eta_c = |\eta_1 - \eta_2| - 2R_c$ , where  $\eta_1$  and  $\eta_2$  are the leading jet rapidities and  $R_c$  is the cone size used to define the jets. For this analysis,  $R_c = 0.7$ , so that  $\Delta\eta_c = |\eta_1 - \eta_2| - 1.4$ . (Events with negative  $\Delta\eta_c$  are not considered.) At a particular cone edge separation the fraction of rapidity gap events can be given by  $f(\Delta\eta_c) = (\sigma_{gap}(\Delta\eta_c) \cdot S) / \sigma(\Delta\eta_c)$ , where  $\sigma(\Delta\eta_c)$  is the total cross section for color-singlet and octet exchange,  $\sigma_{gap}(\Delta\eta_c)$  includes the color-singlet exchange plus octet exchange fluctuations such that nothing inhabits the gap, and  $S$  is the probability that the underlying event does not spoil the gap. This formulation was first suggested by Bjorken [23]. Various theoretical estimates set  $S$  at 10-30%. Therefore, given the ratios cited earlier,  $f(\Delta\eta_c)$  should be on the order of a few percent due to Pomeron exchange [23],[24],[25].

The DØ collaboration has published an upper limit on  $f(\Delta\eta_c > 3)$  for jets with  $E_T$  greater than 30 GeV [26]. Utilizing the hermiticity and segmentation of the calorimeter, the analysis defined a particle as any electromagnetic (EM) tower with more than 0.20 GeV energy. Figure 10 shows the behavior of the fraction of events with no towers above threshold as a function of  $\Delta\eta_c$ . The steep decrease in  $f$  at low  $\Delta\eta_c$  may be ascribed to fluctuations from color-octet exchange filling the gap. At small  $\Delta\eta_c$  there is low probability for soft emission to fill the gap, as  $\Delta\eta_c$  increases the probability will also increase. The color-octet contribution to  $f(\Delta\eta_c)$  vanishes at the higher  $\Delta\eta_c$  [24] and the color-singlet contribution, expected to be flat in  $\Delta\eta_c$ , will dominate [23],[24],[25],[27]. Including systematic errors, at a 95% confidence level and  $\Delta\eta_c > 3$ ,  $f(\Delta\eta_c) < 1.1\%$ . As shown in Fig. 11, this upper limit defines a hyperbola in the  $\sigma_{gap}(\Delta\eta_c) / \sigma(\Delta\eta_c) - S$  plane. The limit, the first quantitative rapidity gap measurement at the Tevatron, severely constrains colorless exchange models.

As first suggested by Bjorken [23], the multiplicity of particles in the rapidity interval provides another picture of rapidity gap events. The top plot in Fig. 12, a histogram from DØ, shows the number of EM towers with more than 0.20 GeV transverse energy for events with jets exceeding 30 GeV  $E_T$  and  $\Delta\eta_c > 3$ . Note the clear excess at low multiplicity. The smooth curve is a negative-binomial distribution fit to the high multiplicity

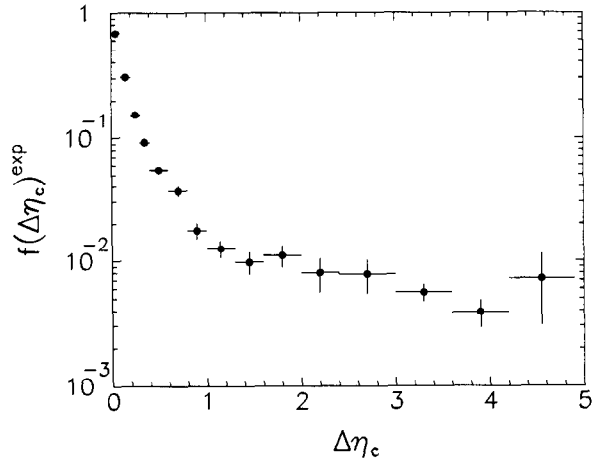


Figure 10: The rapidity gap fraction as a function of rapidity separation. Note the rapid fall-off at low separation and the constant fraction above  $\Delta\eta_c \sim 2$ .

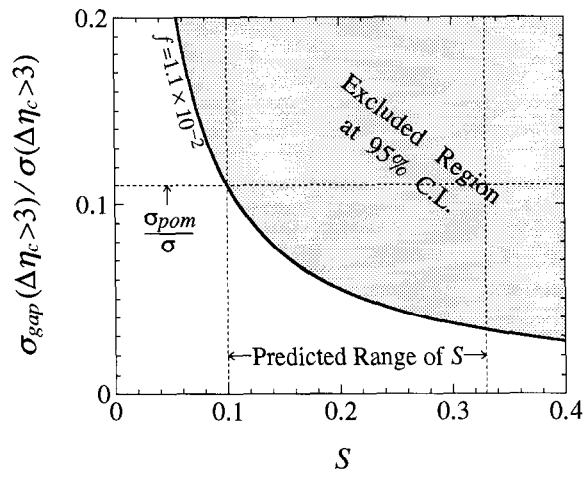


Figure 11: The limit on the rapidity gap fraction expressed in the  $\sigma_{gap}(\Delta\eta_c)/\sigma(\Delta\eta_c) - S$  plane.

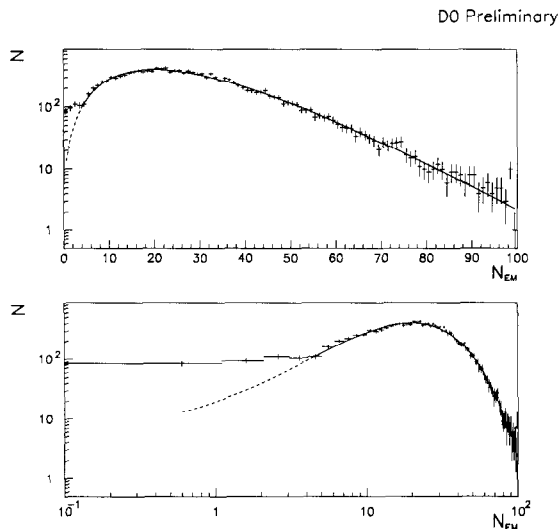


Figure 12: The multiplicity of electromagnetic towers with more than 0.20 GeV transverse energy. The plots are identical except for the logarithmic abscissa.

portion of the histogram. The CDF collaboration has published similar results [28].

Although motivated by theoretical calculations [29] and fragmentation simulations using PYTHIA [30], use of the negative binomial distribution to describe the color-octet contribution in Fig. 12 is better justified by Tevatron jet data. Figure 13 shows the multiplicity distribution for three jet data [31] – dominated by color-octet exchange processes. For the data in this plot,  $\Delta\eta_c > 3$ . The cone edge separation is calculated using the leading jets. The curve is fit satisfactorily with the negative binomial distribution. If the contributions from a third central jet are removed (lower plot Figure 13), the result is also well described by the negative binomial distribution.

Alternately, the control or color-octet sample could require jets on the same side of the detector; for instance both above  $|\eta| > 2$ . This configuration is unlikely to contain any contamination from colorless exchange. In this case, the multiplicity of towers above 0.20 GeV in the central 2.4 units of rapidity is also well described by the negative-binomial distribution (Fig. 14). Any instrumental origin for the excess events at low multiplicities has been ruled out.

The lower plot of Fig. 12 is a double logarithmic representation of the  $\Delta\eta_c > 3$  multiplicity distribution [31]. This presentation clearly illustrates a  $1.4 \pm 0.2\%$  excess above the negative binomial distribution at low multiplicities. The excess is consistent with

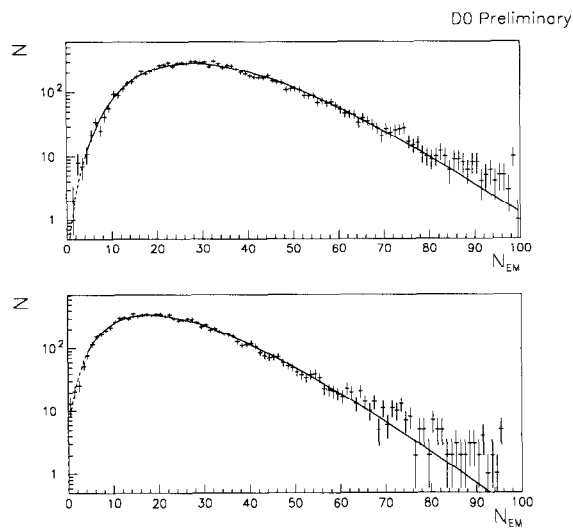


Figure 13: The electromagnetic tower multiplicity for three jet events. The top plot includes contributions from all three jets. The bottom plot excludes contributions from the central, third jet.

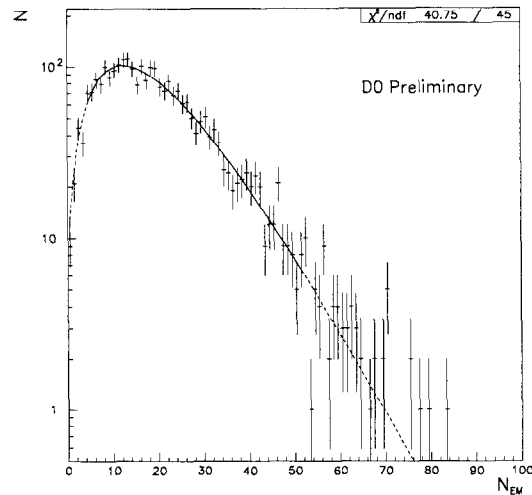


Figure 14: The central tower multiplicity distribution for two forward jets.

colorless exchange. CDF’s published value, to be described later in these proceedings by Dino Goulianos, is in good agreement with the 1.4% excess [28].

## 5 Inclusive Photon Cross Section and “ $k_T$ ”

Direct photon production at the Tevatron is dominated for  $E_T \sim 10\text{-}50$  GeV by Compton scattering,  $qg \rightarrow q\gamma$  or  $\bar{q}g \rightarrow \bar{q}\gamma$ , and is therefore quite sensitive to the gluonic content of the proton. Higher order bremsstrahlung graphs, for instance  $qg \rightarrow qg$  where the final state quark radiates a photon, also provide beyond-leading-order tests of QCD. The pdf and higher order calculation tests available with photon production measurements are very similar to those of dijet production.

The inclusive photon measurement of  $G(x)$  is free of uncertainties due to jet energy scale or parton fragmentation. The measurement does suffer one important drawback: the signal must be extracted from the large  $\pi^0$  and  $\eta$  meson decay background. There are several methods employed to reduce or estimate the background and details can be found in the references [32],[33]. Nevertheless, because the photon and jet based measurements have very different systematic errors, they provide important cross-checks to the derivation of  $G(x)$ .

The inclusive photon cross section as measured by CDF is shown in Fig. 15. Also shown is a NLO QCD prediction using the CTEQ2M pdf [32]. The cross section, restricted to  $|\eta_\gamma| < 0.9$ , falls over four orders of magnitude from 10 to 120 GeV/c  $p_T$ . At similar  $p_T$  the photon cross section is very roughly three orders of magnitude below the jet cross section. The inset shows the cross section utilizing two independent methods of background estimation. Figure 16 shows the percentage difference between the data and theory. The agreement is good above  $\sim 30$  GeV/c but there seems to be an excess of production at the lowest  $p_T$ . The DØ data shows no significant deviation from NLO at any  $p_T$ [33].

The CTEQ collaboration has noted an excess of photon production at low  $x$  in nearly all the direct photon data accumulated over the last ten years. Figure 17 plots the percentage difference between the NLO prediction using CTEQ2M for an impressive array of results [7]. At the lowest  $x$  accessible by each experiment there appears to be excess production. A NLO prediction using all the photon data to determine the pdf shows nearly identical behavior [7].

A possible origin of the excess, as suggested by CTEQ, could be higher order processes

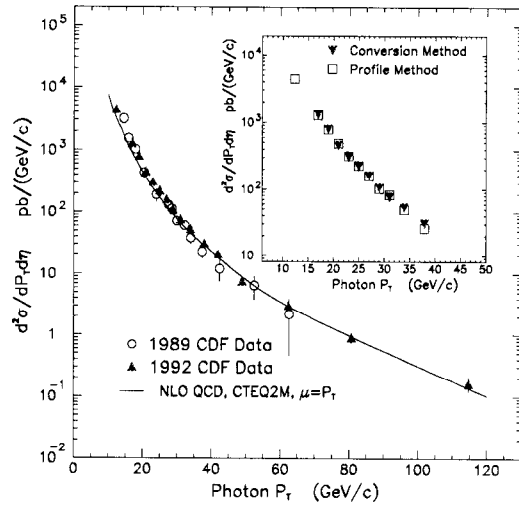


Figure 15: The central inclusive photon cross section as a function of photon  $p_T$ . The inset shows the cross section utilizing two different methods of background subtraction.

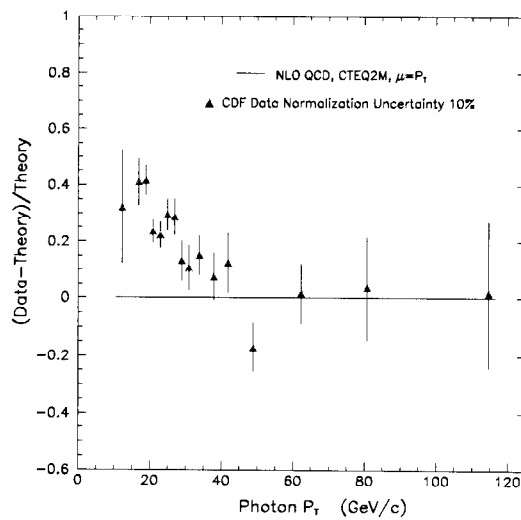


Figure 16: The difference as a function of  $p_T$  between the photon data and a NLO QCD calculation.

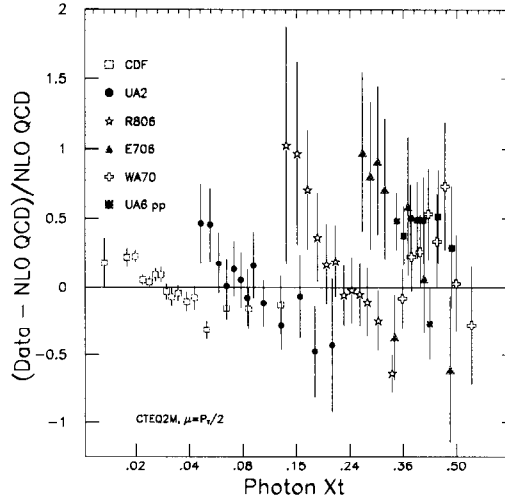


Figure 17: A compilation of photon production measurements compared to a NLO QCD calculation. Note that the prediction disagrees with most experimental results at the lowest  $x$  obtained by each experiment.

which impart transverse momentum or “ $k_T$ ” to the initial partons. The presence of such transverse momenta on the observed cross section would be profound. Since the  $k_T$  would be misinterpreted as  $p_T$ , the observed cross section as a function of  $p_T$  would be a smeared version of the true cross section as a function of  $p_T$ . The high cross section at lower  $p_T$ , say 5 GeV/c, would make a large contribution at higher  $p_T$ 's. Supporting evidence for nonzero  $k_T$  can be found in diphoton production data. In all cases, the average  $p_T$  of the diphoton system is nonzero. At the Tevatron the average is  $\sim 4$  GeV/c [34]. Simulations with PYTHIA show this to be the correct magnitude required to explain the excess production at low  $p_T$ [7]. This is most assuredly an interesting observation; higher order calculations may be required to explain these results.

## 6 The Measurement of $\alpha_s$ from $W + jet$ Production

To lowest order,  $W$  production involves only an electroweak vertex and is unaccompanied by jets. When a single jet is produced through annihilation ( $q\bar{q}' \rightarrow Wg$ ) or Compton scattering ( $qg \rightarrow W\bar{q}'$ ), an additional factor of  $\alpha_s$  enters the picture. Thus, the ratio of the  $W + 1jet$  cross section to  $W + 0jet$  cross section can provide a measure of  $\alpha_s$ .

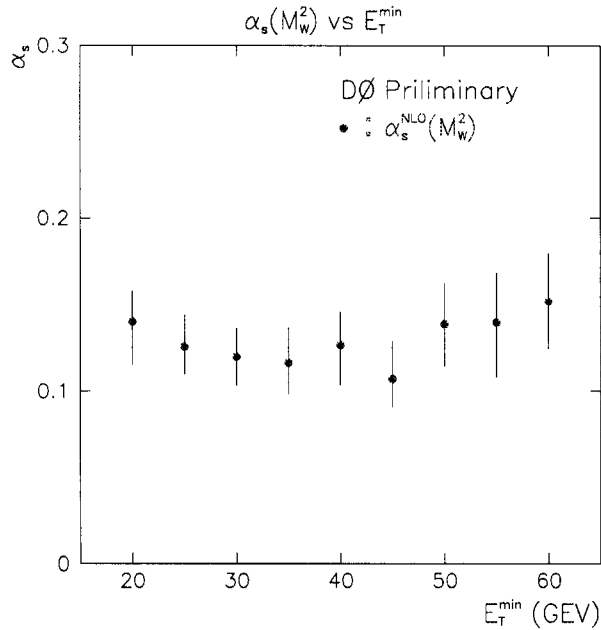


Figure 18: The strong coupling constant as measured by the  $W + 1jet$  to  $W + 0jet$  ratio as a function of minimum jet  $E_T$ . Errors shown are statistical only and correlated bin-to-bin.

Past measurements of  $\alpha_s$  from  $W + jet$  production have suffered from large uncertainties due to uncalculated higher order processes [35]. With the advent of NLO predictions (i.e.  $q\bar{q}' \rightarrow Wgg$ ) these uncertainties have been greatly minimized [8]. In addition, because the calculations include two final state gluons or quarks, a jet finding algorithm can be approximately implemented at the theoretical level. The ratio of the number of  $W + 1jet$  events to  $W + 0jet$  events,  $R$ , can now be calculated as a function of any algorithm parameters. For the cone algorithm these would be the cone size,  $R_c$ , and the minimum jet transverse energy,  $E_{Tmin}$ . The effect of the experimental choices may be folded into the theoretical predictions through use of a Monte-Carlo simulation [8]. The precise relationship between  $\alpha_s$  and  $R(R_c, E_{Tmin})$  is given by the NLO calculation [8].

As shown in Fig. 18, a preliminary result from D0, the derived value of  $\alpha_s$  is, indeed, independent of the choice of  $E_{Tmin}$  and yields  $\alpha_s = 0.123 \pm 0.015$ . Analysis details can be found in the references [36]. The measurement error is dominated by the uncertainty in the jet energy scale. There is also a theoretical contribution to the error dominated by the choice of pdf used in the NLO calculation. The D0 collaboration will publish final results soon.

## 7 Conclusions

As the results presented here demonstrate, NLO QCD describes most aspects of central jet, photon and  $W$  production. There are interesting deviations at the highest jet and lowest photon  $E_T$  values which will require more data and time to explain. Because NLO calculations are generally accurate, the pdf's are now under intense scrutiny at the Tevatron. As the CDF and DØ triple differential jet cross section analyses mature, they should provide information for the determination of  $G(x)$ . Taken together with the photon results these will place stringent constraints on  $G(x)$ . Interestingly, as hinted by the inclusive photon cross sections, perhaps higher order processes incorporating transverse momenta of the partons may be required to fully describe the photon data.

A new avenue of study, jet production at large separation, has opened up access to higher orders of jet production. Two extreme analyses, dijet decorrelation and the search for rapidity gaps have already revealed much about higher order QCD. At least with current statistics and at the rapidity separations yet examined, GLAP evolution describes most aspects of decorrelation. The observation of rapidity gaps, signals for colorless exchange, provides a new and particularly interesting handle on strong interactions. To round out our study of QCD, the program at FNAL has also provided the first measurement of  $\alpha_s$  from the Tevatron.

In closing, the study of QCD at FNAL has been invigorated by recent experimental and theoretical advances. At last count there were over fifty QCD studies of which only a small sample were discussed here. The future remains bright, as nearly  $200 \text{ pb}^{-1}$  of data will be collected in 1995 and 1996. To add to the richness of this data set, some of that luminosity may be recorded at one and perhaps two lower center of mass energies, 630 and 1200 GeV.

## References

- [1] S. Abachi *et al.* (DØ Collaboration), "The DØ Detector", NIM A**338** 185 (1994).
- [2] F.Abe *et al.*, Nucl. Instrum. Methods Phys. Res., Sect. A**271**, 376 (1988) and references therein.
- [3] S.Ellis *et al.*, Phys. Rev. Lett. **64** 2121 (1990).

- [4] W.Giele, E.W.N.Glover, and David A. Kosower, “The Two-Jet Differential Cross Section at  $O(\alpha_s^3)$  in Hadron Collisions”, FERMILAB-PUB-94/070-T (1994).
- [5] V.Del Duca and C.R.Schmidt, “Dijet Production at Large Rapidity Intervals”, Phys. Rev. D**49** 4510 (1994); DESY preprint 94-144 (1994).
- [6] M.Derrick *et al.* (ZEUS Collaboration), DESY preprint 94-192 (1994); I.Abt *et al.* (H1 Collaboration), Phys. Lett. B**321** 161 (1994); G.Rädel, *Proc. 27th Int. Conf. on High Energy Physics*, Glasgow, July 1994, eds. P.J.Bussey and I.G.Knowles.
- [7] J.Huston *et al.* (CTEQ Collaboration), “A Global QCD Study of Direct Photon Production”, Michigan State University preprint MSU-HEP-41027 and CTEQ preprint 407 (1994).
- [8] W.T.Giele, E.W.N.Glover, and D.A.Kosower, Nucl. Phys. B**403**, 633 (1993).
- [9] T.Åkesson *et al.* (AFS Collaboration), Phys. Lett. B**123** 133 (1983).
- [10] J.Alitti *et al.* (UA2 Collaboration), Phys. Lett. B**257** 232 (1991).
- [11] F.Abe *et al.* (CDF Collaboration), Phys. Rev. Lett. **61** 613 (1988); F.Abe *et al.* (CDF Collaboration), Phys. Rev. Lett. **68** 1104 (1992).
- [12] F.Aversa, *et al.*, Phys. Rev. Lett. **65** 401 (1990).
- [13] E.Kovac *et al.* (CDF Collaboration), “Testing QCD with Jet Physics at CDF”, Fermilab preprint FERMILAB-Conf-94/215-E, (1994).
- [14] V.D.Elvira (DØ Collaboration), “Inclusive Jet Cross Sections at the DØ Detector”, Fermilab preprint FERMILAB-Conf-94/323-E (1994).
- [15] A.Arnison *et al.*, Phys.Lett. B**136**, 294 (1984); P.Bagnaia *et al.*, Phys.Lett. B**144**, 283 (1984).
- [16] F.Nang (DØ Collaboration), “Measurement of the Triple Differential Inclusive Dijet Cross Section”, Fermilab preprint FERMILAB-Conf-94/323-E (1994).
- [17] A.D.Martin *et al.*, “Pinning down the Glue in the Proton” Rutherford Appleton Laboratory preprint RAL-95-021 and University of Durham preprint DTP/95/14 (1995).

- [18] W.J.Stirling, "Production of Jet Pairs at Large Relative Rapidity in Hadron-Hadron Collisions as a Probe of the Perturbative Pomeron", Nucl.Phys. B**428** 3 (1994).
- [19] G.Marchesini and B.R.Webber, Nucl.Phys. B**310** 461 (1988).
- [20] T.Heuring (DØ Collaboration), "Jet Production at Large Rapidity Intervals", Fermilab preprint FERMILAB-Conf-94/323-E (1994).
- [21] Y.Dokshitzer, V.Khose, and S.Tryon, *Proc. of the 6th Int. Conf. on Phys. in Collisions* (1986), ed. M.Derrick (World Scientific, Singapore, 1987).
- [22] R.S.Fletcher and T.Stelzer, Phys. Rev. D**48**, 5162 (1993).
- [23] J.D.Bjorken, Phys.Rev. D**47**, 101 (1992).
- [24] H.Chehime *et al.*, Phys. Lett. B**286**, 397 (1992).
- [25] E.Gotsman,E.M.Levin and U.Maor, Phys. Lett. B**309**, 1993 (1993).
- [26] S.Abachi *et al.* (DØ Collaboration), Phys. Rev. Lett. **72** 2332 (1994).
- [27] V.Del Duca and W.K.Tang, SLAC preprint SLAC-PUB-6310 (1993).
- [28] F. Abe *et al.* (CDF Collaboration), Phys. Rev. Lett. **74**, 855 (1995).
- [29] I.Dremin, submitted to Physics Uspekhi, FIAN TD-6, (1994) and references therein.
- [30] R.Fletcher, private communication.
- [31] B.May (DØ Collaboration), "Rapidity Gaps Between Jets at DØ ", Fermilab preprint FERMILAB-Conf-94/323-E (1994).
- [32] F.Abe *et al.* (CDF Collaboration), Phys. Rev. Lett. **73**, 2662 (1994).
- [33] S.T.Fahey (DØ Collaboration), "Direct Photon Production at DØ ", Fermilab preprint FERMILAB-Conf-94/323-E (1994).
- [34] F.Abe *et al.* (CDF Collaboration), Phys. Rev. Lett. **70**, 2332 (1993).
- [35] J.Alitti *et al.*, Phys.Lett. B**263**, 563 (1991); M.Lindgren *et al.*, Phys. Rev. D**45** 3038 (1992).
- [36] J.Kotcher (DØ Collaboration), "Measurement of the Strong Coupling Constant ( $\alpha_s$ ) Using  $W + jets$  Processes in the DØ Detector", Fermilab preprint FERMILAB-Conf-94/323-E (1994).